International Journal of u- and e- Service, Science and Technology
Vol.8, No. 11 (2015), pp.303-316
http://dx.doi.org/10.14257/ijunesst.2015.8.11.30

A Study on the Approach of the Structured Light Three-dimensional Measurement

Wang beiyi, Yu xiaoyang*, He baohua, Cai yingfu, Zhang jixun and Sun Xiaoming

The higher educational key laboratory for Measuring & Control Technology and Instrumentations of Heilongjiang province, Harbin University of Science and Technology, Harbin 150080, China
yuxiaoyang@hrbust.edu.cn

Abstract

In order to establish the 3D Temperature Field based on structure light 3D measurement and cross-correlation registration. Infrared/Visible camera calibration method and heterologous images registration method were studied. First, according to infrared camera's characteristics, the selection of calibration templates have been studied and the calibration of the infrared camera has been accomplished on the basis of planar calibration method; then, we simplified the two-step method based on the mature principle of structure light measurement; and the visible camera was calibrated; finally, use calibrated visible cameras to form structured light measurement system, and register the infrared image and visible image in the geometrical position. Experimental results show that: the relative error of measurement system is less than 0.3%;infrared and visible image's alignment error in geometrical position is 0.0015 mm. and measurement systems have good reconstruction results for plane and curved ,and cross-correlation method has a good effect for heterrologous images registration.

Keywords*: structure light; infrared camera; calibration; registration*

1. Introduction

The technology of 3D temperature field involved in the field of military, medical and industrial production.IR camera is not affected by the light environment during operation, and the object can be measured around the clock; visible camera is restricted by the light when it works, but visible images have high contrast and high resolution features, it's easy to have access to the characteristics of the surface feature information, Registration technology of homologous image has been fully developed, but these registration method's effect when dealing with heterologous image are not very satisfactory. In forging industrial production, high temperatures will cause the material to undergo complex physical and chemical changes,the size of the change in the process has a direct impact on the structural performance and accuracy class, constructing 3D temperature field for real-time measurement ,in order to achieve online monitoring, has important economic significance for industrial production.

In other countries, in2011, Michael Gschwandtner, Roland, Kwitt, Andreas Uhl and Wolfgang Pree proposes a self-calibration method including visible camera and infrared camera[1],which is extended on the traditional camera calibration method. And the method can be useful for IR camera calibration. For the visible camera calibration, the method use a classic chessboard template and an algorithm [2] proposed by Zhang Zhengyou in 2000 to obtain the visible camera's intrinsic parameters; For infrared camera calibration, the method use the original chessboard template with the array of resistor that

ISSN: 2005-4246 IJUNESST

can release infrared radiation, so that the calibration plate is visible to the infrared camera, and become a template for infrared camera calibration.

2012, Stephen Vidas and Ruan Lakemond etal proposed an calibration mothod for single infrared camera and multiple infrared camera[3]. This method homemade a calibration template: a grid consisting of a series of opaque rectangles and a background with different radiation levels. It has been testified that the calibration template is clearer than heating chessboard in the infrared camera.

In China, Li Chenglong proposed a infrared camera self-calibration system [4]. The method uses a multi-camera dynamic calibration method to calibrate the intrinsic parameters and extrinsic parameters of one or more infrared cameras. Firstly it needs projective reconstruction, and then reconstruct conduct Euclidean reconstruction according to the intrinsic parameters of infrared camera, so you can get all camera's projection matrix of calibration system in the same world coordinate system, and then decompose them into the intrinsic parameters and extrinsic parameters. After experiment, the accuracy of the calibration method is higher than the number of the existing methods, in addition, the difficulty of the calibration method is relatively low, relatively easy to operate.

There are also a lot of depth and meticulous research in the image registration.

In foreign countries, Moravec presents a gray scale of auto-correlation coefficients to distinguish between a relationship between the area and the area of the pixel, which is a classic feature point detection [5] in 1977. Harris operator[6] proposed by Harris C. and MJ Stephens in 1988 is a feature point extraction operator, which is the improvement of the Moravec corner detection algorithm, using first-order partial derivatives to describe the brightness changes, this operator inspired by the auto-correlation function in the signal processing, the matrix M is given and linked to autocorrelation function. Eigen values of the matrix M is a first-order curvature of the auto-correlation function, if the two curvature values are high, the point is the feature points.

David G lowe proposed a local feature description operator based on scale space (SIFT, scale invariant feature transform) [7] detecting the feature point, SIFT operator detects the potential feature points for scale and rotation invariant by Gaussian differential functions in scale space. The algorithm was gradually improved in 2004.

In China, Zhu Yinghong, Li Junshan *et al.*, proposed a point matching algorithm based on shape context. first, feature points are extracted by the curvature scale space(CSS)[8]corner detector; and then choose normal direction of feature points as the main direction; and search for the feature points on the same edge; depend on the histogram of similarity neighborhood to construct the descriptor, and be normalized. Finally, complete the matching of feature points by the nearest neighbor algorithm.

Wang Song proposed a bilateral matching algorithm based on sift operator feature point detection and applying KD-tree and quasi-Euclidean distance[9]. This registration method using two different registration threshold, carrying reverse registration after forward registration; using the quasi-Euclidean distance has the advantages of more feature points, higher registration accuracy, the drawback is that registration is slow.

Ma proposed a pretreatment method [10] that enhancing image edge firstly, and then histogram equalization, finally using matching strategy of gray correlation.

Above proposed method is broadly divided into two categories: template-based registration algorithm and feature-based registration algorithm. for heterologous image, because of their feature vector's directions are different, the computation of the selected feature points is complexity; while infrared image general is considered to be the negative image of the visible image, so describing its gray information is more convenient method than feature points after preprocessing visible image, so the text will be taken after gray mutual information method for registration.

2. Infrared Cameras and Visible Camera Calibration Theory and Experiment

2.1. Principle of Visible Camera Calibration

1) Algorithm Analysis

Two-step calibration method is that: ignoring lens error, then using the intermediate variable calibration equations into linear equations about extrinsic parameters camera system, again to solve the intrinsic parameters of the system. This method can not only simplify the calculation model, but also improve the measurement accuracy. In this paper, monocular coplanar lattice produced a calibration plate, the specific calibration steps is that: projector projects to template calibrate with the coding pattern, and the camera get pictures after rendering. Then using Matlab writes calibration procedures, including image binarization, calculate the distance between measuring points, the image coordinate calculation and calibration procedures. According to the two-step calibration method we can calculate the intrinsic and extrinsic parameters of the camera, camera calibration is complete.

2) Verification Experiment

Place a spotlight In the world coordinates(0,0,0), and place a camera in the world coordinates(400,0,0), set the resolution at $N^c \times M^c = 1024 \times 768$, focal length f=49.455mm, it is assumed to be an ideal environment, so the camera lens hole model for ignoring lens distortion and deformation angle $\alpha = 90o$. Matlab programming calculated calibration results, compared with the standard values listed in table here, in order to compare the calibration results with Calib_box. The comparison results are shown in Table 1-1.

Table 1. The Comparison between Two-step Calibration Value and the Standard Value

Calibration parameters	Standard value	Calibration values	Measurement error	Calibration parameters	Standard value	Calibration values	Measurement error
f_x	49.455	49.396	0.059	R_{33}	0	0	0
f_y	49.455	49.396	0.059	R_{31}	-0.342	-0.342	0
R_{11}	0.94	0.94	0	R_{32}	0	0	0
R_{22}	0	0	0	R_{33}	0.934	-0.934	0
R_{33}	0.342	0.342	0	T_1	0	0.056	0.152
R_{21}	0	0	0	T_2	50	50.000	0
R_{22}	1	1	0	T_3	-584.76	-584.165	0.595

Through calculating the data in the table, you can get lens focal length maximum relative error of 0.11% maximum relative error of the intrinsic and extrinsic parameters is 0.10%. The camera lens in the measurement is approximately holes model, so the lens distortion coefficients are approximately zero.

2.2. Infrared Camera Calibration Principle

1) Algorithm Analysis

Zhang Zhengyou proposed a flexible infrared camera calibration method that can easily calibrate the camera in 1998, the camera only needs to observe a number of a planar pattern displayed in different directions (at least two). The camera or the planar pattern can move freely without needing to know how to exercise. Zhang Zhengyou builds a model for radial lens distortion, and the program contains the analytical solution and subsequent nonlinear optimization algorithm based on maximum likelihood criterion. We used simulations and real data to test this new technology, and received very good results. As in the past the use of expensive equipment, such as the typical technology about two or three orthogonal planes, compared to this new technology is more practical and flexible.

The algorithm is as follows: two-dimensional point with a three-dimensional point of use, we use the augmented vector expressed it by adding 1 as the last element:. General pinhole camera model: the relationship between M and its three-dimensional point of the two-dimensional projection between points m has been given by:

$$s\tilde{m} = A[R, t]\tilde{M} \qquad \text{with } A = \begin{bmatrix} \alpha & \gamma & u_0 \\ 0 & \beta & v_0 \\ 0 & 0 & 1 \end{bmatrix} \tag{1}$$

Where s is an arbitrary scale factor, R and t are the extrinsic parameter which associates with the world coordinates and the camera coordinate, and A is called the camera intrinsic matrix,α and β the scale factors in image u and v coordinate axis ,and γ the parameter describing the skew of two axes.

if the plane model of the image is given, we can estimate the homography. Since a homography is determined by 8 degrees of freedom and six extrinsic parameters, we can get two constraints for intrinsic parameters:

$$H_1^T A^{-T} A^{-1} h_2 = 0 \tag{2}$$

$$H_1^T A^{-T} A^{-1} h_1 = H_2^T A^{-T} A^{-1} h_2 \tag{3}$$

A^{-T} and A^{-1} actually describe the absolute conic of images. By these two constraints can solve parameters.

So:

$$B = A^{-T}A^{-1} = \begin{bmatrix} B_{11} & B_{12} & B_{13} \\ B_{21} & B_{22} & B_{23} \\ B_{31} & B_{32} & B_{33} \end{bmatrix} = \begin{bmatrix} \frac{1}{\alpha^2} & -\frac{\gamma}{\alpha^2\beta} & \frac{u_0\gamma - u_0\beta}{\alpha^2\beta} \\ -\frac{\gamma}{\alpha^2\beta} & \frac{\gamma}{\alpha^2\beta} + \frac{1}{\beta^2} & -\frac{\gamma(u_0\gamma - u_0\beta)}{\alpha^2\beta^2} - \frac{v_0}{\beta^2} \\ \frac{u_0\gamma - u_0\beta}{\alpha^2\beta} & -\frac{\gamma(u_0\gamma - u_0\beta)}{\alpha^2\beta^2} - \frac{v_0}{\beta^2} & \frac{(u_0\gamma - u_0\beta)^2}{\alpha^2\beta^2} + \frac{v_0^2}{\beta^2} + 1 \end{bmatrix} \tag{4}$$

The inversion of B can obtain the intrinsic parameters matrix A, then A can calculate the extrinsic parameter matrix corresponding to each image.

2) Calibration Experiments

There is a big difference between the imaging principle of infrared cameras and visible cameras. Almost the feature is very obvious in the view of the human eye .But in the infrared camera it is not easy to show up, Figure 1 are resultant images of the calibration board by visible camera and an infrared camera.

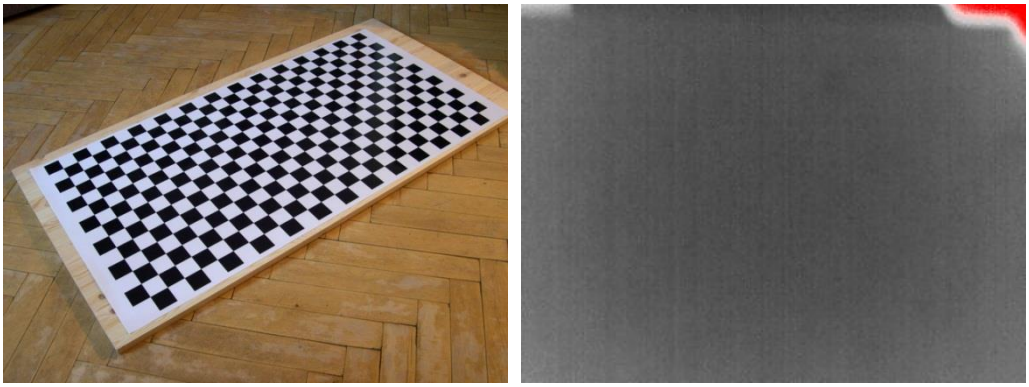

Figure 1. Calibration Board Taken by Visible Camera and Infrared Cameras

For this feature, we have made changes to the calibration board, due to pictures in part of the high temperature is highlight, and it is approximately white after binarization, so we make white checkered chessboard calibration hollow-out, and placed a heat radiation in the back of the calibration board, so that the heat radiation can transmit though the hollow-out, while retaining the black box can block heat radiation. Figure 2 is infrared camera calibration diagram; Figure 3 is visible camera and infrared camera renderings renderings after hollow-out.

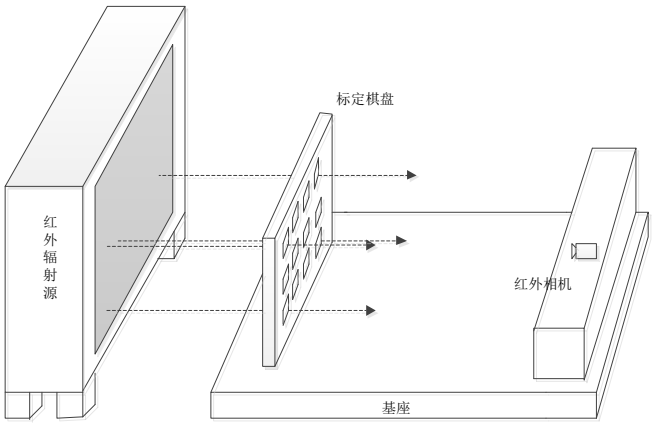

Figure 2. Infrared Camera Calibration Diagram

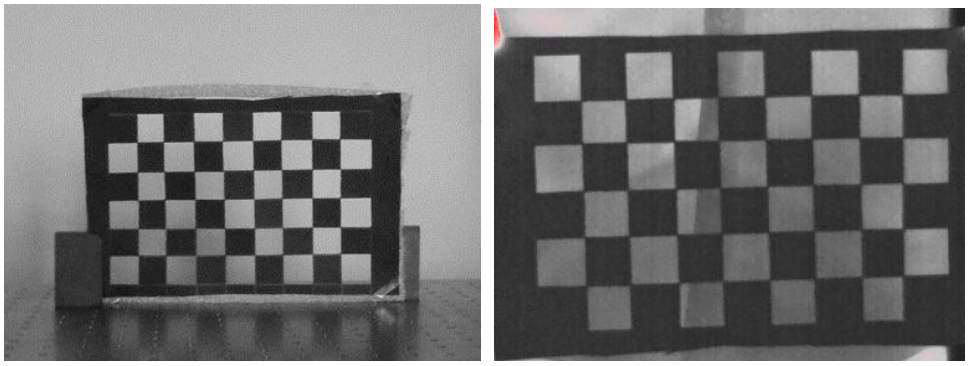

(a) (b)

Figure 3. Shooting Effect Comparison

Use Calib toolbox to read images and extract the corner, the results shown in Figure 4:

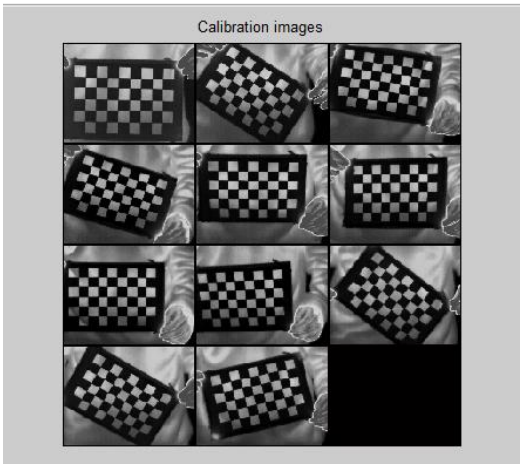

Figure 4. Corner Extraction Results

And outputs the result as follows:

$$f_c = [1405.929 \quad 1399.547] ? [270.804 \quad 269.776]$$

$$c_c = [180.893 \quad 194.567] ? [27.839 \quad 37.692]$$

$$alpha_c = [0.000 \quad 0.000]$$

$$k_c = [-3.367 \quad 75.737 \quad -0.0463 \quad -0.0383 \quad 0.000]$$

$$err = [0.685 \quad 0.757]$$

That:

$$A_c = \begin{bmatrix} 49.388 & 0 & 512.748 \\ 0 & 49.500 & 384.890 \\ 0 & 0 & 1 \end{bmatrix}$$

We can get reprojection of each board position in Matlab, as shown in Figure 5:

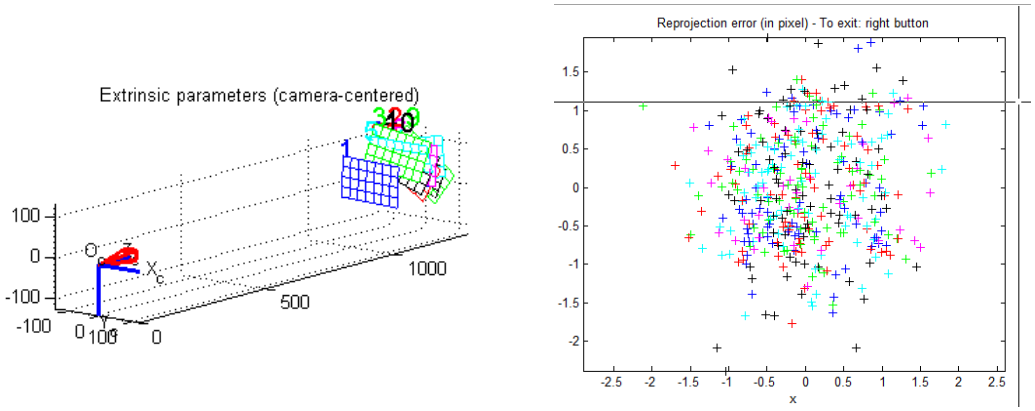

Figure 5. Reprojection and Error Analysis Results

According to the image, we can observe that the calibration error is relatively large, which is relative about the bent of calibration board, after removing gross error, error pixel of X / Y axis are controlled within two pixels.

We only need one picture when using calib_toolbox to calibrate extrinsic parameter.

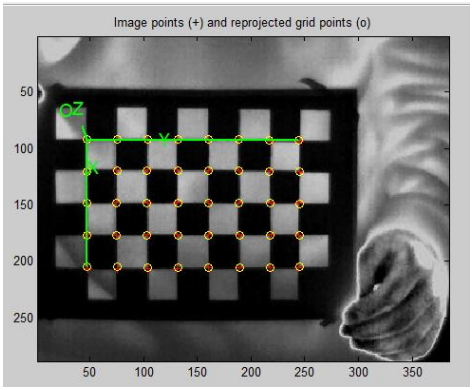

Figure 6. Extrinsic Parameter Calibration

Extrinsic calibration parameters results as follow:

$$T_c = \begin{bmatrix} -110.120 & -83.824 & 1230.613 \end{bmatrix}$$

$$R_c = \begin{bmatrix} 0.002 & 0.998 & 0.055 \\ 0.999 & 0.000 & -0.028 \\ -0.028 & 0.055 & -0.998 \end{bmatrix}$$

$$err = \begin{bmatrix} 0.635 & 0.748 \end{bmatrix}$$

3. 3D Measurement Experiments after Visible Camera Calibration

The following will simulate the measurement for flat and curved, to achieve the purpose of validating the calibrated visible camera parameters. Set a spotlight in world coordinates(0,0,0),with a resolution of 1024 × 768, and set a different projection mapping; place a camera in the world coordinate (400,0,0) at a resolution of 1024 × 768, focal length 49.455mm; and place a object in the measuring range.

1. Plane Measurement

Place a vertical plane at 300×200mm in the measurement system which has been established. Within the measuring range at 430-570mm, range in the depth value at intervals of 20mm for variation multiple measurements , and determines the change of the error in the measurement process. The experimental procedure taking 430mm depth values as a starting point will place the vertical plane in the measured depth value point and put nine encoded image sequentially irradiated onto the plane and were taken with the camera, the image was calculated through the measurement procedures written by Matlab and got 3D information. Such objects can be drawn by measuring extreme values on each axis.

At X-axis, the maximum value of measuring is 149.871mm and the minimum is -149.302mm; At Y-axis, the maximum and minimum values are 100.291mm; Through simple calculation,we can obtain that the length of plate is 299.173mm, and height is 200.582mm. And the result of depth error is calculated for each point, and get that the maximum measurement error is 1.051mm when the depth is 430mm, the average measuring error is 0.415mm and the relative maximum error is 0.24%.

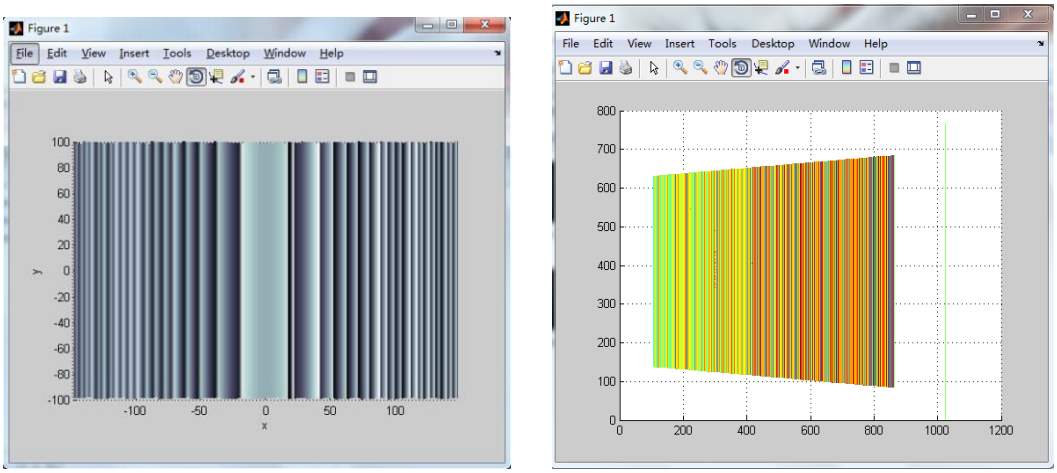

Figure 7. Reconstruction Results and Measurement Error

The following will measure the plane at 20mm intervals, to calculate the maximum measurement error, the relative maximum error and the average error. Table 3-1 shows the results of a total of eight experimental measurement locations within the 430-570mm.

Table 2. Depth Value Measurements in 430-570mm

Depth	430	450	470	490	510	530	550	570
The maximum measurement error	1.051	1.162	1.228	1.311	1.458	1.558	1.583	1.720
The maximum relative error	0.24	0.26	0.26	0.27	0.29	0.29	0.29	0.3
The average error	0.415	0.447	0.478	0.516	0.557	0.594	0.632	0.680

We can find that the measurement error is incremented by the table, so as the same manner, with a depth value at 430mm as a starting point, move the plate back at per 20mm intervals to measure it, the camera view cannot fully accommodate the plane, and data cannot be measured.

2. Surface Measurement

This section will measure the surface of the sphere, reconstruct the surface and calculate. Set a sphere with a diameter of 100mm in the world coordinates (200, 480, 0), Measured the sphere according to the method of plane measurements. Figure (a) is the measurement error of the surface of the sphere; Figure (b) the reconstruction results of a sphere when a depth value is 480mm.

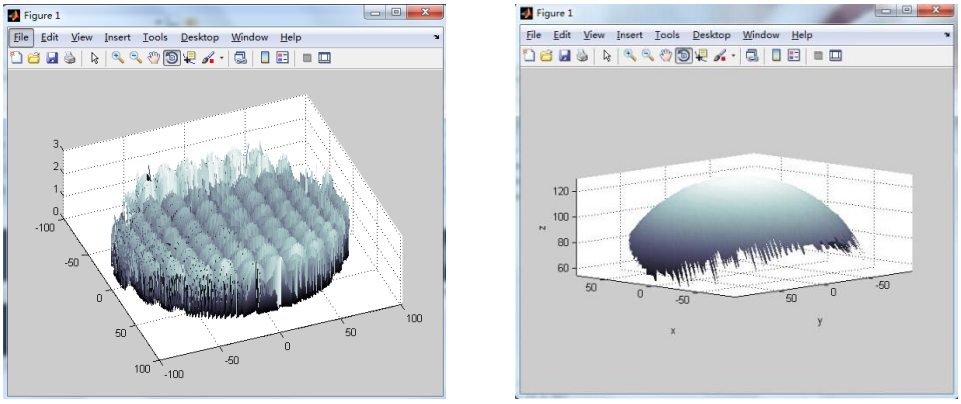

(a)The Measurement Error (b) The Reconstruction Results of a Sphere

Figure 8. Reconstruction Results and Measurement Error

It can be calculated that maximum measurement error is 2.593mm and the average measurement error is 0.764mm. Similarly, repeated measurements at the radius of the sphere 20mm intervals and calculates the average error and the maximum error of the measurement. The experimental results are shown in Table 3-2.

Table 3. Measurements within Sphere of Radius is 80-130mm

Measuring the radius/mm	80	90	100	110	120	130
The maximum measurement error/mm	3.240	5.038	2.593	2.523	2.480	2.510
The average error/mm	0.701	0.727	0.764	0.815	0.869	0.918

From the above results it can be seen, the calculated by three-dimensional coordinate information may contain gross errors. In the measurement error analysis diagram, you can clearly see that this part of the gross errors are mostly concentrated in the edge of the measuring object, which is affected by the edge curvature of the measured object, resulting in the program will appear error decoding. The gross error is obvious in the measurement of cone.

4. The Experimental Infrared Camera Calibration after Registration

Mutual information refers to any variable information and another any variable information has many common parts. Principle of mutual information registration means what extent about an image's information and another image's information is consistent, that is to say, this principle is statistical correlation corresponds to gray value of visible image and infrared image. The definition of entropy is a statistics, used to measure random of the variables. The randomness of a variable is greater, the greater its entropy. According to the definition of entropy and joint entropy is:

$$MI(A, B) = H(A) + H(B) - H(A, B) \tag{5}$$

As known from the above equation when the H (A) and H (B) obtain the maximum value and the H (A, B) obtain the minimum value, the registration of the two is completed. Figure 9 using Venn diagram expressed the relationship between various kinds of entropy and mutual information.

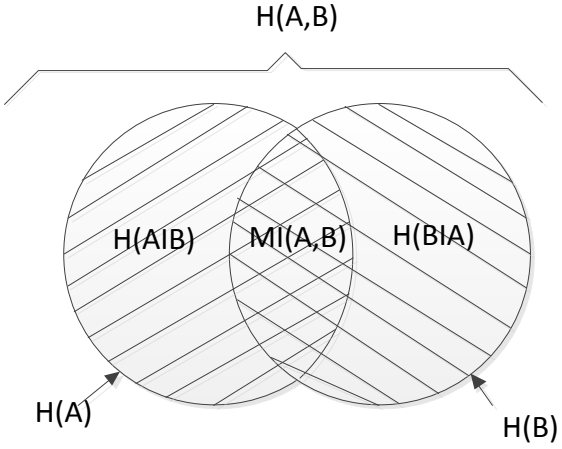

Figure 9. Relationship between Entropy and Mutual Information

The above analysis briefly explains the principle of mutual information registration. The following work applied it to register the infrared image and visible image.

Through the observation of the two images in Figure 10, we can clearly find white pixels in the infrared image focused on high temperature objects, which is on the contrary with the visible image, so next we need to carry on processing to the visible image.

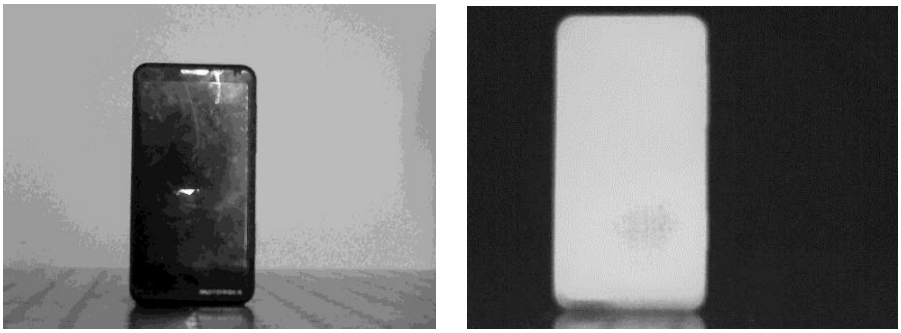

Figure 10. Comparison of Visible Image and Infrared Image

Due to differences in the two image's intensity, we use an anti-color image of visible image. After inverting processing, gray distribution of visible image and infrared image is similar in part of the region, in order to highlight the edges, and further use histogram equalization, processing effect as shown in Figure 11.

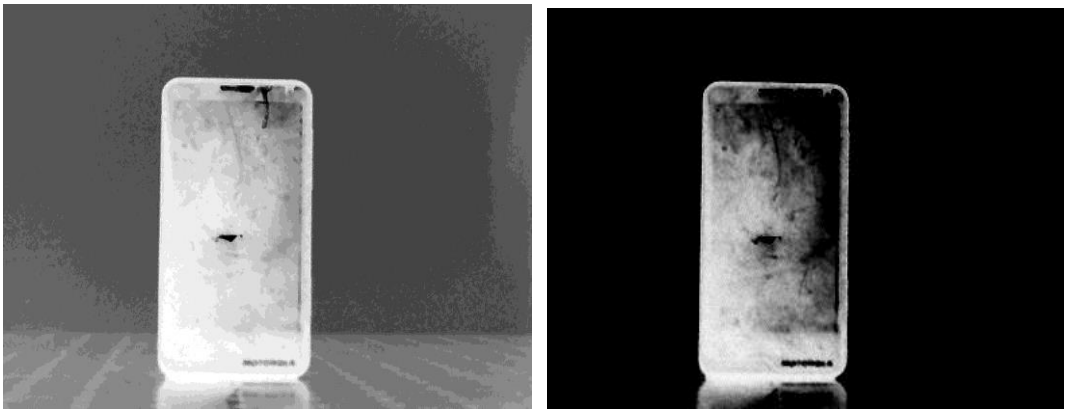

Figure 11. Pretreatment Results

After a series of treatment, compare the visible light image and infrared image, the white pixels of the visible image are concentrated within the outline of objects, and outside of the outline does not exist the white pixels, which is identical with the infrared image. Registration difficulty at this time will be greatly reduced. Next, use mutual information image to register the two images.

Registration work is still using GUI functionality on the MATLAB platform, simply enter registration and reference images in the interface can automatically complete the search and integration work. After entering the pretreatment visible and infrared image's grayscale, the program will automatically complete the registration, the registration parameters are as follows:

$$X, Y, Angle = [18.033][38.004][-0.015]$$

$$MI_{value} = [0.947]$$

Figure 12 is a fusion of the image registration:

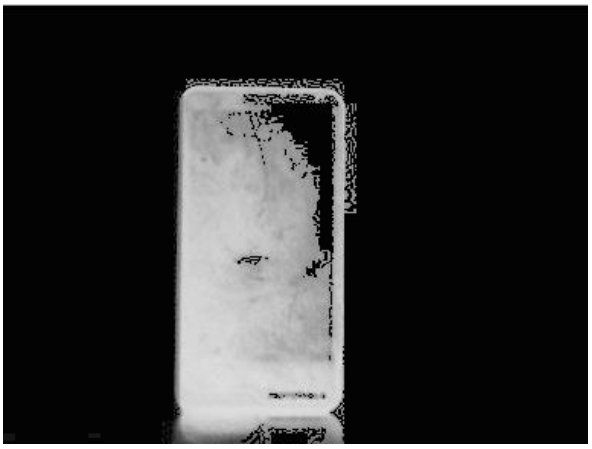

Figure 12. Grayscale Image after Registration

From the fusion picture we can see that registration between the infrared image's left edge and visible image is completed, and image exceeds the edge on the right side and the upper side. This is due to the different camera resolution caused by different objects in the image geometry size. Although the registration has many problems, basically completed the prototype registration work, I will learn in the future to further improve the work.

5. Conclusion

This paper completed the calibration work of visible light camera and infrared camera, and compared with the setting parameters, the experimental results show that: the maximum relative error of the lens focal length is 0.11%, the maximum relative error of intrinsic and extrinsic parameters is 0.10%. The experimental results are quickly and accurate. After the completion of the calibration, planar and curved surface were measured using the 3D measuring system; finally tried to use the mutual information registering heterogonous image.

After more in-depth research, this study still needs further exploration, the next step work should first focus on forming binocular measurement in the application of infrared camera and visible camera, further exploring the registration algorithm of infrared image and visible image, and completing construction of 3D temperature field.

Acknowledgments

This work is supported by the National Natural Science Foundation of China (61401126).

References

[1] M. Gschwandtner and R K. Witt, "Infrared Camera Calibration for Dense Depth Map Construction", IEEE Intelligent Vehicles Symposium (IV), **(2011)**, pp. 857-861.
[2] Z. Zhang, "A Flexible New Technique", .IEEE Transactions on Pattern Analysis and Machine Intelligence, vol. 11, no. 22, **(2000)**, pp. 1330-1334.
[3] Vidas, Stephen and Lakemond, "A mask-based approach for the geometric", IEEE Transactions on Instrumentation and Measurement, no. 61, **(2012)**, pp. 1265-1365.
[4] C. Li, "Research based on three-dimensional reconstruction method of infrared thermal image", Anhui University, **(2013)**.

[5] M. Wu and K. Gong, “Some discussion on moravec operator”, China science and technology achievements, no. 16, **(2011)**, pp. 62-65.
[6] M. Li and L. Zhu, “The Approach of Feature Point Detection for Illumination Pattern-based Images under Bias Field”, Hangzhou, **(2006)**.
[7] D. G. Lowe, “Distinctive Image Features”, Vancouver, B.C., Canada:University of British Columbia, **(2004)**, pp. 2-6.
[8] Y. Zhu and J. Li, “A feature point description and matching algorithm for edge in IR/visual image”, Journal of Computer-Aided Design & Computer Graphics , vol. 25, no. 6, **(2013)**, pp. 858-864.
[9] J. Ma, “A scene matching approach based on edge signal between IR and visible image”, The Huazhong University of Science and Technology ,**(2006)**.
[10] S. Wang, “SIFT based image matching algorithm research”, Xidian University, **(2013)**.

